forests

Article

New Data on Phytochemical and Morphophysiological Characteristics of *Platycladus orientalis* L. Franco and *Thuja occidentalis* L. Conifer Trees in Polluted Urban Areas of Kazakhstan

Nurgul Yerezhepova [1], Meruyert Kurmanbayeva [1,*], Nina Terletskaya [1,2], Moldir Zhumagul [1,3,4], Marko Kebert [5], Milena Rašeta [6], Yusufjon Gafforov [7,8,9], Roza Jalmakhanbetova [10] and Medeu Razhanov [4]

1 Faculty of Biology and Biotechnology, Department of Biodiversity and Bioresources, Al-Farabi Kazakh National University, Al-Farabi Av. 71, Almaty 050040, Kazakhstan; nkaznu@gmail.com (N.Y.); teni02@mail.ru (N.T.); mzhakypzhan@mail.ru (M.Z.)
2 Institute of Genetic and Physiology, Al-Farabi Av. 93, Almaty 050040, Kazakhstan
3 Higher School of Natural Sciences, Astana International University, Qabanbay Batyr Ave 8, Astana 020000, Kazakhstan
4 Astana Botanical Garden Branch of the Republican State Enterprise on the Right of Economic Management "Institute of Botany and Phytointroduction" of the Committee of Forestry and Wildlife of the Ministry of Ecology, Geology and Natural Resources of the Republic of Kazakhstan, Orynbor 16, Astana 020000, Kazakhstan; m.razhanov@mail.ru
5 Institute of Lowland Forestry and Environment, University of Novi Sad, Antona Čehova 13d, 21000 Novi Sad, Serbia; kebertmarko@gmail.com
6 Department of Chemistry, Biochemistry and Environmental Protection, Faculty of Sciences, University of Novi Sad, Trg Dositeja Obradovića 3, 21000 Novi Sad, Serbia; milena.raseta@dh.uns.ac.rs
7 Central Asian Center for Development Studies, New Uzbekistan University, Tashkent 100000, Uzbekistan
8 Department of Education and Training Management, Tashkent International University of Education, Tashkent 100207, Uzbekistan
9 Institute of Botany, Academy of Sciences of Republic of Uzbekistan, Tashkent 100125, Uzbekistan
10 Department of Chemistry, Faculty of Natural Sciences, L.N. Gumilyov Eurasian National University, Astana 010000, Kazakhstan; rjalmakhanbetova@gmail.com
* Correspondence: kurmanbayevakz@gmail.com

Abstract: The adaptive potential of plants in urban environments, responding to factors like air pollution, electromagnetic radiation, and specific microclimates, remains insufficiently understood. Our study focused on two evergreen *Cupressaceae* family species, *Thuja occidentalis* L. and *Platycladus orientalis* L. Franco, which are commonly found in Kazakhstan's urban landscapes. Conducted in Almaty, one of Kazakhstan's most polluted cities, our comparative analysis examined the anatomical features, photosynthetic activity, and secondary metabolite composition of these conifers. Both species exhibited xeromorphic traits, such as submerged stomata, resin passages, and a prominent leaf cuticle. *T. occidentalis* displayed higher photosynthetic activity values (quantum yield of photosystem II (YII), electron transport rate (ETR), and quantum yield of non-photochemical quenching (Y(NPQ))) than *P. orientalis*, while *P. orientalis* exhibited a higher quantum yield of non-regulated energy dissipation in PSII (Y(NO)) values. Chemical analysis revealed 31 components in *T. occidentalis* and 33 in *P. orientalis*, with *T. occidentalis* containing three times more thujone (16.42% and 5.18%, respectively) and a higher monosaccharide content (17.33% and 6.98%, respectively). *T. occidentalis* also contained 14.53% steroids, whereas *P. orientalis* showed no steroid presence. The cytotoxic activity of essential oils was determined by the survival of *Artemia salina* aquatic crustaceans, whereas tested essential oils from both species exhibited acute lethal toxicity to *A. salina* aquatic crustaceans across all tested concentrations. The connection between physiological traits, adaptation strategies, and cytotoxic effects offers a comprehensive view of the ecological and pharmacological importance of these two observed conifer species, highlighting their diverse roles in urban environments, as well as their potential medical uses.

check for updates

Citation: Yerezhepova, N.; Kurmanbayeva, M.; Terletskaya, N.; Zhumagul, M.; Kebert, M.; Rašeta, M.; Gafforov, Y.; Jalmakhanbetova, R.; Razhanov, M. New Data on Phytochemical and Morphophysiological Characteristics of *Platycladus orientalis* L. Franco and *Thuja occidentalis* L. Conifer Trees in Polluted Urban Areas of Kazakhstan. *Forests* **2024**, *15*, 790. https://doi.org/10.3390/f15050790

Academic Editor: José Javier Peguero-Pina

Received: 2 April 2024
Revised: 23 April 2024
Accepted: 24 April 2024
Published: 30 April 2024

Keywords: anatomical structure; *Artemia salina*; chemical composition; *Cupressaceae*; cytotoxic activity; GC/MS analysis

1. Introduction

The impacts of global warming and the resulting climate change extend beyond natural forests to encompass urban forests and parks [1]. Compared to their natural equivalents, urban forests are expected to be disproportionately vulnerable to heat waves, largely due to the prevalence of phenomena like urban heat islands (UHI), which unavoidably compromise human health in urban settings [2]. Urban heat islands are produced due to the numerous sun reflections off of surfaces like asphalt and buildings composed of materials with high thermal conductivity, as well as traffic congestion [3]. In addition to heat stress [4], a variety of abiotic stressors are recognized in urban environments, including drought [5], salinity [6], and the presence of various pollutants, including heavy metals [7] such as xenobiotics, including persistent organic pollutants (POPs) like polycyclic aromatic hydrocarbons (PAHs) [8] and polychlorinated biphenyls (PCBs), all of which pose significant threats to tree survival in urban areas. In addition to adversely impacting human health, all of these pollutants pose a threat to the sustainability of ecosystem services provided by urban tree species to residents of urban environments. These ecosystem services include air purification, noise reduction, temperature regulation and urban cooling, shade provision, runoff mitigation, stormwater management, carbon sequestration, recreational and health benefits, etc. [9].

Almaty, Kazakhstan's largest urban center, is renowned as one of the nation's most polluted cities, particularly described as an air pollution "hotspot" due to the presence of NO_2 emissions [10,11]. The city grapples with elevated levels of atmospheric pollutants, including $PM_{2.5}$, PM_{10}, SO_2, NO_2, and CO, which often surpass recommended limits, posing significant health risks [10]. An analysis from 2013 to 2017 reveals a noteworthy rise in annual PM_{10} concentrations, while NO_2 and SO_2 levels fluctuate, and CO shows a declining trend, indicative of evolving emission sources, potentially from enhanced public transportation and increased coal combustion [10].

Pollution sources in Almaty stem from vehicle emissions, coal-fired combined heat and power plants (CHPs), construction, and residential coal burning, exacerbated by the city's mountainous terrain, trapping stagnant air and prolonging pollution exposure. Driven by the urgent need to mitigate air pollution's adverse effects on health, productivity, and overall well-being, Almaty's response includes measures like enhanced air quality monitoring, cleaner fuel adoption in CHPs, the promotion of public transit, and the transitioning of households from coal to gas heating. Despite stable atmospheric conditions for much of the year, pollutant concentrations show a weak correlation with meteorological factors [10].

Urban parks in Almaty, serving as "green oases" within the city landscape, exemplify ecosystems modified by human activity, offering various ecosystem services and additional benefits, notably aesthetic appeal [12].

Another concept and ecosystem service of significant importance, yet to be fully elucidated, pertains to the emission of volatile organic compounds (VOCs) from trees, particularly conifers [13]. Apart from their role in allelopathic communication in regards to plant–plant interaction and repellent or attractant activities among plants and insects, volatile organic compounds (VOCs) also exert notably beneficial effects on humans, functioning as antimicrobial, antioxidant, anti-inflammatory, antiviral, and anticancer agents [14,15]. Therefore, the ability of different tree species to adapt to future altered climate scenarios is crucial for both the stability of urban forest ecosystems and the sustainability of these ecosystem services, as well as for the understanding of the underpinning mechanism of adaptation in order to identify climate-ready tree species [16,17].

Conifer trees play a vital role in urban landscaping, primarily due to their evergreen nature, which enhances their visual attractiveness. However, conifers are particularly susceptible to air pollution owing to the prolonged longevity of their foliage [18]. Nonetheless, specific species of coniferous trees demonstrate resilience to urban conditions [16].

Among the numerous forest species that enhance urban forest ecosystem services, *Platycladus orientalis* L. Franco and *Thuja occidentalis* L. stand out for their aesthetic appeal, decorative value, and their abundant phytochemical composition [19]. *T. Occidentalis,* or Northern white cedar, historically utilized by Indigenous peoples of North America for medicinal purposes, notably for treating respiratory ailments and skin conditions, while modern medicine has confirmed a wide range of diverse therapeutic potentials, including antimicrobial, antiviral, antifungal, antioxidant, and anti-inflammatory properties [19]. *T. occidentalis* stands out as a valuable source of its predominant compound, the monoterpene α-thujone, which has demonstrated efficacy against malignant glioblastoma multiforme cells [19] and shows promise as an active agent against polycystic ovary syndrome [20]. On the other hand, *Platycladus orientalis* L. Franco, or Chinese thuja, is also a conifer tree species valued for both its ornamental and medicinal properties due to its high levels of compounds such as α-thujone, α-cedrol, camphor, and cineole, which contribute to its effectiveness in treating respiratory and skin ailments [21]. In this study, the authors opted to analyze *T. occidentalis* and *P. orientalis* due to their specific attributes. Particularly, *T. occidentalis* is recognized for its capacity to endure high levels of pollution [22,23], while *P. orientalis*, akin to *T. occidentalis*, is notably favored for urban planting, showcasing a substantial lifespan exceeding 50 years [24]. Despite being widely planted as ornamental trees in Kazakhstan, both in public spaces and private gardens, comprehensive and thorough research on their anatomical, morphological, and phytochemical characteristics remains notably lacking.

The process of extracting essential oils is an intricate craft, with the quality of the oil influenced by numerous factors, including plant species, genotype, the plant organ selected for extraction, the extraction method and conditions employed, the distillation parameters, and environmental conditions [25]. A well-established phenomenon in plant biology is the “stress-induced essential oil production”, wherein it has been demonstrated that both the qualitative and quantitative chemometric properties of essential oils exhibit significant variation when plants are pre-exposed or “primed” to either biotic or abiotic stressors, such as elevated temperature or drought [26,27]. This behavior is attributed to the stimulation of secondary metabolite biosynthesis caused by stress factors, while concurrently, stress impedes biomass production, frequently due to inadequate water content in the plant tissues [28].

Urban environments, characterized by elevated temperatures, heavy metal, and persistent organic pollutant (POPs) contamination, intensified traffic, and industrial air pollutants, impose significant pressures on plants to adapt, particularly by affecting their anatomical features, and through the modulation of their photosynthetic activity to ensure survival and normal functioning [29]. Anatomical and morphological adaptations, such as leaf xerophytization, aim to optimize moisture use by urban plants, which is particularly crucial when physiological processes slow down under stress [30]. Photosynthetic activity, a key criterion for adaptation, directly impacts plant growth and development and is among the primary processes negatively affected by stress [31].

To best of our knowledge, there is a lack of information regarding the response of *Platycladus orientalis* and *Thuja occidentalis* conifer trees to urban stresses in the polluted areas of Kazakhstan. Hence, the primary aim of this study was to evaluate how the demanding urban conditions in Almaty, Kazakhstan, affect the adaptive abilities of these two conifer species, *T. occidentalis* and *P. orientalis*, including the following:

A. Morpho-anatomical characteristics;
B. Gas exchange properties and chlorophyll fluorescence;
C. Essential oil chemical composition and their cytotoxicity, evaluated through the mortality of *Artemia salina* larvae.

2. Materials and Methods

2.1. Study Area

The city of Almaty is situated at the geographic coordinates of 77° E and 43° N, centrally located in the southeast Kazakhstan. Nestled in the foothills of the northern slope of the Zailiisky Alatau mountain system within the Northern Tien Shan, the city covers a total area exceeding 170 square kilometers. During the mid-2000s, urban areas in the foothills experienced the extensive construction of high-rise buildings, leading to a significant obstruction of the natural airflow from the mountains [10]. The geographical location and topography of Almaty impose limitations on the vertical dispersion of pollutants, thereby contributing to substantial air pollution levels [10].

2.2. Plant Material

Thuja occidentalis L., a charming small tree, is cultivated in Almaty, Kazakhstan, particularly along Al-Farabi Avenue within the grounds of Al-Farabi Kazakh National University, located at coordinates 43°13.480′ N 76°55.359′ E. Originally a key element in the ancient sacred garden tradition of the Far East, the tree was introduced to Europe in 1752 for ornamental purposes and has been naturalized in some regions. Commonly found in parks and gardens, it also thrives in natural settings on limestone cliffs and walls, displaying remarkable adaptability to air pollution, drought, and challenging climates. *Platusladus orientalis* L. Franco has also been cultivated within the premises of Al-Farabi Kazakh National University, situated at coordinates 43°13.307′ N 76°55.396′ E, in Almaty, Kazakhstan. In our investigation, we sourced plant specimens from a total of 30 individuals belonging to *T. occidentalis* and *P. orientalis*, specifically choosing 15 plants of each species. From each plant, we collected three samples during the period spanning 2018 to 2022. The herbarium specimens of these plants are archived in the herbarium collection of the Astana Botanical Garden (NUR), identified by the numbers NUR0006840-NUR0006842.

2.3. Morpho-Anatomical Observation

Young leaves from generative plants were selected for anatomical analysis, with samples obtained from 15 individuals of each species, replicated three times. The plant material underwent a month-long immersion in a solution composed of alcohol, glycerin, and water in a 1:1:1 ratio. Leaf sections were prepared using a microtome MZP-01 (“Technom”, Ekaterinburg, Russia), equipped with a freezing unit OL-ZSO 30 (“Inmedprom”, Yaroslavl, Russia). The sections were subsequently encapsulated in glycerol. Examinations and measurements of the anatomical features in the prepared leaf sections were conducted using a Micro Opix MX 700 (T) microscope (West Medica, Wiener Neudorf, Austria). Microphotographs were captured using a Cam V1200C HD (West Medica, Wiener Neudorf, Austria).

2.4. Chlorophyll Fluorometers Study

To assess chlorophyll fluorescence, 15 leaves were sampled from each species. The measurements were conducted using a Junior-PAM device (Heinz Walz GmbH, Effeltrich, Germany) with an RLC 450 Nm actinic light. The middle one-third portion of the leaf, known for its homogeneous ChFP distribution, was used for fluorescence measurement. The measurements were performed on bright days between 9 a.m. and 11 a.m. The leaves were shaded before recording the light response curve. Considering the challenge of achieving complete darkness in the field, the initial state was considered quasi-darkness. Eight saturation pulses of 10,000 μmol/m^{2}s were applied every 20 s, while actinic light increased from 0 to 625 μmol/m^{2}s. Using WinControl-3.29 software, parameters such as the maximum quantum yield of PSII (Fv/Fm), the effective photochemical quantum yield of PSII (Y(II)), the quantum yield of regulated energy dissipation (Y(NPQ)), the quantum yield of non-regulated energy dissipation (Y(NO)), and the relative electron transport rate of PSII (ETR) were calculated.

2.5. Non-Targeted Metabolomic Analysis of Essential Oils by Using Gas Chromatography Coupled with Mass Spectrometry Detection

The extraction of organic compounds involved immersing a 10 g plant sample into 50 mL of 96% ethanol and mixing for 12 h in the dark using a magnetic stirrer. Separation and identification of the extracted compounds were conducted using an Agilent 6890N/5973N chromatography-mass spectrometer (Santa Clara, CA, USA), with periodic ion scanning. A sample volume of 1.0 µL was injected at a temperature of 240 °C, without flow separation. Separation was achieved using a DB-WAXetr chromatographic capillary column (Santa Clara, CA, USA). The temperature program applied was as follows: the initial column temperature was set at 50 °C for 5 min, followed by heating at a rate of 50 °C/min to 300 °C. Detection was performed in SCAN mode in the m/z range of 34–750. The Agilent MSD ChemStation software, version 1701EA controlled the process. Data processing, including identification of retention times, peak areas, and spectral information, utilized the Wiley 7th edition and NIST'02 libraries for decoding mass spectra. In addition, the isolation of volatile constituents involved hydrodistillation using a Clevenger apparatus.

2.6. Cytotoxicity Assay

The dividing funnel is charged with artificial seawater (55 mL), and *Artemia salina* eggs (200 mg) undergo processing and are stored for 3 days with a gentle air supply until larvae emerge. One side of the funnel is shielded with aluminum foil. After 5 min, the larvae congregated on the illuminated side of the funnel are extracted using a Pasteur pipette. Approximately 20–40 larvae are distributed into each of the 24 wells containing 990 mL of seawater. Dead larvae are enumerated under a microscope. A 10 mL DMSO solution is added to the 10 mg/mL sample. The reference drugs are actinomycin D or staurosporine, while the negative control receives treatment solely with 10 µL of DMSO. Following 24 h incubation and an additional 24 h storage period to ensure immobility, the deceased larvae are tallied under a microscope.

Mortality (P) was determined by the following formula:

$$P = (A - N - B)/Z \times 100, \quad (1)$$

A—number of dead larvae after 24 h;
N—number of dead larvae before the test;
B—the average number of dead larvae in the negative control;
Z—the total number of larvae.

2.7. Statistical Analysis

Statistical assessments were carried out utilizing IBM SPSS statistical software, version 19.0 (IBM Corp., Armonk, NY, USA). Each experiment was replicated three times, and the results were presented as the mean ± standard deviation (SD). Microsoft Excel was employed for data manipulation and analysis. Outliers were identified and removed using t-test outcomes, while the standard error of the mean sample was computed.

3. Results and Discussion

3.1. Morpho-Anatomical Characterization

Thuja occidentalis displayed scale-like leaves arranged in tight rows along its branches, forming a flat spray in which the leaves extensively overlapped, covering the branch almost entirely. Numerous stomata were present on the abaxial side of the leaf, submerged and covered by stomatal cells, with the guard cells completely open.

An examination of the anatomical structure of the *T. occidentalis* leaves revealed that the outer epidermal walls feature a thick cuticle, particularly on the abaxial side, consisting of slightly sinuous cell walls followed by a hypodermis layer. Secretory ducts on the abaxial side were positioned directly beneath the hypodermis. Below the hypodermis were parenchymatous mesophyll cells with characteristic ridge-like invaginations, containing chloroplasts and resin cavities. Mesophyll cells exhibit heteromorphism in the main veining area. The endoderm surrounds the main conductive bundle, which is amphicribral, with the xylem surrounding the phloem (Figure 1). Transition tissue surrounds the vascular bundle, comprising tracheids and parenchyma cells, some with intercellular spaces. Lateral conductive bundles are collaterally closed, with outward-directed xylem and centrally directed phloem. The average size of the xylem vessels was 19.68 ± 1.45 µm. Idioblasts in the outer phloem sharply differ from the surrounding cells in shape and size, with most bioactive substances concentrated around the phloem (Figure 1).

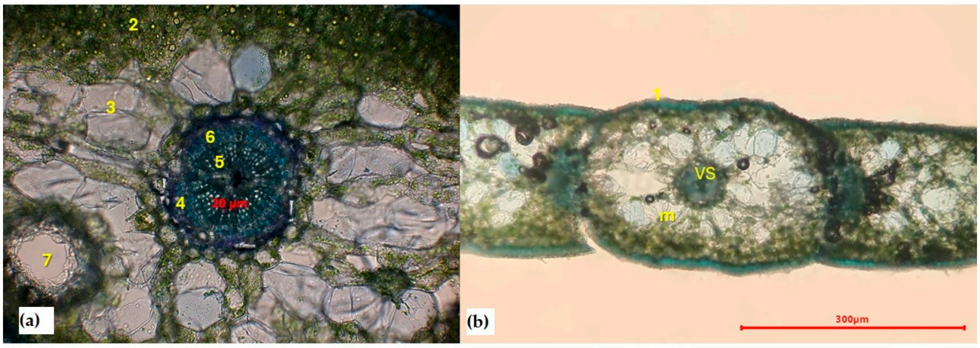

Figure 1. Cross section of the three scale-like leaves of *T. occidentalis*, revealing photosynthetic tissues and vascular bundles. (**a**) The scale bar represents 20 µm, indicating the magnification level of the image. (**b**) The scale bar represents 300 µm, indicating the magnification level of the image. This scale range (20–300 µm) allows for a better understanding of the size and structure of the observed anatomical features. The central leaf is rounded, and the two marginals are elongated. (1) The epidermis consists of a single cell layer, with thickened cell walls and a cuticle. The mesophyllum (m) is heterogenous. (2) The adaxial side comprises chlorenchyma with 2–3 cell layers, characterized by small, rounded cells containing numerous chloroplasts. (3) The inner part of the mesophyllum has large parenchymatic cells and intercellulars that are linked to the chlorenchyma with narrow bridges of small chlorenchymatic cells. (4) Surrounding the vascular bundle (VS), the innermost cell layer of the mesophyll consists of a single layer. The vascular bundle consists of (5) xylem (tracheids) in the inner region and (6) phloem (sieve cells) in the outer region. (7) Resin ducts are also evident.

The leaves of *P. orientalis* exhibited a compound leaf structure with characteristic dimorphism on the flat part of the axis. Two types of leaves were present: facial leaves and lateral leaves. Both types were scale-like, and stomata are found on the undersides of both facial and lateral leaves.

An examination of the anatomical structures of *P. orientalis* leaves revealed that the outer walls of the upper and lower epidermal cells featured a cuticle, but lacked trichomes. Stomata on the leaf lamina were slightly bent inwards. Beneath the epidermis was the hypodermis. On the adaxial side of the leaf, the palisade mesophyll consisted of three rows of columnar cells with abundant chlorophyll grains, and a large resin passage was located between the palisade mesophyll cells. On the abaxial side, the spongy mesophyll comprised loose parenchyma cells with numerous air spaces. In the cross-section of the facial leaf, the main conductive bundle was surrounded by the endoderm, with cells of various sizes. Parenchymal cells surrounded the endoderm. In the center, there was a concentric amphivasal type conductive bundle, where the phloem surrounded the xylem (Figure 2).

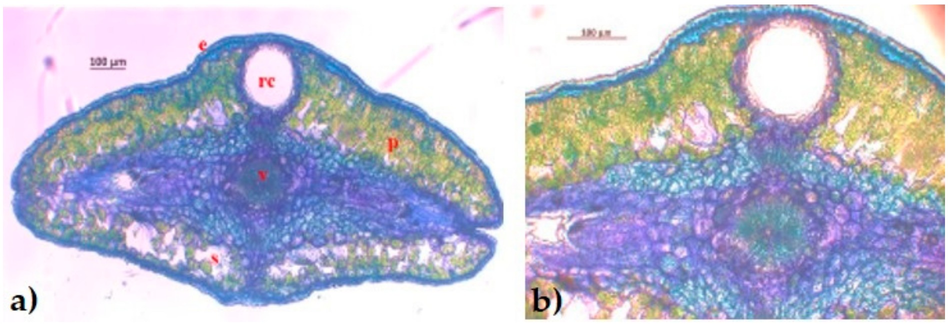

Figure 2. Cross section of a facial leaves of *P. orientalis*: e—epidermis; p—palisade mesophyll cell; s—spongy mesophyll cell; v—vein; rc—resin channel. (**a**) The scale bar represents 100 µm, indicating the magnification level of the image. (**b**) The scale bar represents 130 µm, indicating the magnification level of the image. This scale range (100–130 µm) allows for a better understanding of the size and structure of the observed anatomical features.

In the cross-section of a lateral leaf of *P. orientalis*, starch crystals were observed, and biologically active substances were present in the mesophyll, along with yellow essential oils. The diameter of the main conductive bundle in the lateral leaf of *P. orientalis* was measured at 119.16 ± 28.42 µm. The conductive bundle displayed a collateral arrangement, with the phloem extending towards both the adaxial and abaxial sides, while the xylem pointed towards the center. Parenchymal cells were also present. The main conductive bundle comprised 37–40 rays of the xylem, with a phloem-to-xylem ratio of 67%. Additionally, a single resin passage, measuring 50.63 ± 17.31 µm in diameter, was identified (Figure 3).

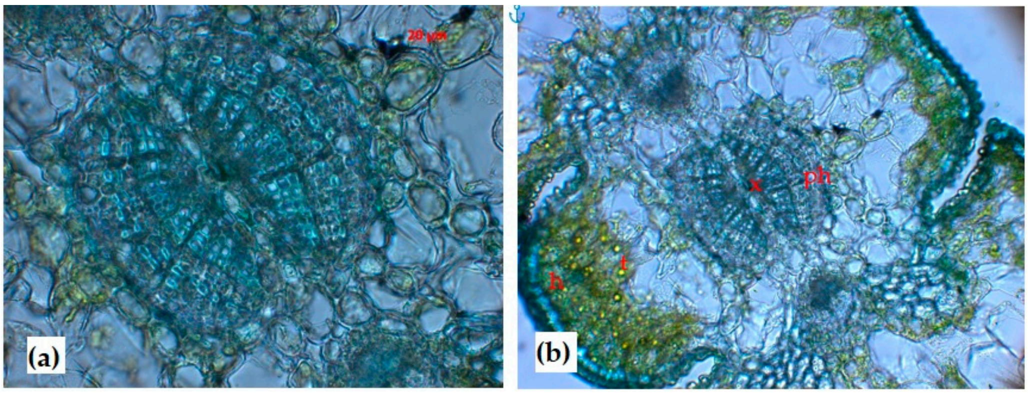

Figure 3. Cross section of the facial leaves of *P. orientalis*. Letters in the images indicate the following: h—hypoderm; t—tannin; x—xylem; ph—phloem. (**a**) The scale bar represents 20 µm, indicating the magnification level of the image. (**b**) The scale bar represents 100 µm, indicating the magnification level of the image. This scale range (20–100 µm) allows for a better understanding of the size and structure of the observed anatomical features.

The two sampled species, *T. occidentalis* and *P. orientalis*, exhibited distinctive xeromorphic traits, such as submerged stomata and resin passages, contributing to the maintenance of ecophysiological activity at a stable level. The well-developed leaf cuticle serves a protective function, while epicuticular wax mitigates damage to the photosynthetic apparatus and reduces heat load through light reflection [32]. Parenchyma cells, with their pronounced expression, play crucial roles in wound healing, regeneration processes, and the short-range transport of dissolved substances [33]. These cells exhibit a resumption of meristematic activity when exposed to artificially altered environments, highlighting the plants' ability to adapt to adverse conditions while preserving their life potential [34–36].

Biologically active compounds are likely found on the outer side of the phloem, with a concentration around the conductive bundle. Specifically, the cells surrounding the idioblasts likely showed a concentration of bioactive compounds, while cells with pronounced white changes were observed, particularly around the resin passage. Furthermore, tannins were likely observed surrounding the conductive bundles on both sides above the phloem.

3.2. Photosynthetic Properties

The values of YII, ETR, and Y(NPQ) were higher in *T. occidentalis* compared to *P. orientalis*, while the values of the parameter Y(NO) were higher in *P. orientalis* than in *T. occidentalis* (Figures S1–S4).

The examination of the "light curves" revealed that the photosynthetic activity of the *T. occidentalis* leaves surpassed that of *P. orientalis*. This superior photosynthetic performance and the enhanced photoprotective mechanisms in *T. occidentalis*, as indicated by higher values of key photosynthetic parameters, contribute to our understanding of the photosynthetic characteristics of these plant species. These findings indicate implications for their adaptability and resilience in diverse environmental conditions.

The regulation of photosynthetic electron transport is crucial to prevent the accumulation of damaging byproducts of oxygen and reactive oxygen [37]. The higher values of Y(II) and ETR in *T. occidentalis* may be linked to the more effective activation of non-photochemical quenching (NPQ) mechanisms in this species, suggesting its greater photosynthetic potential compared to *P. orientalis*. NPQ plays a role in plant adaptation to various stress factors and is a primary component of acquired systemic resistance [38,39]. It can compensate for a decrease in Y(II) and even lead to a decrease in Y(NO) [40]. NPQ activation involves the dissipation of excess excitation energy, the regulation of photosynthetic electron flow, and the prevention of harmful singlet oxygen $^1O_2$ formation, thereby preventing oxidative damage to the leaves [31,39,41,42]. Consequently, higher Y(NPQ) values and lower Y(NO) values in *T. occidentalis* compared to *P. orientalis* indicate a relatively high level of photosynthetic activity in this species. Recognizing that NPQ serves as a mechanism for protecting plants against photooxidative stress by dissipating excessive light energy as heat, while also involving the conversion of violaxanthin to zeaxanthin, *T. occidentalis* exhibited greater adaptability to stress conditions when compared to *P. orientalis* [43]. The Y (NPQ) values found for *T. occidentalis* are similar to those previously reported by Orekhhov et al. [44].

3.3. Phytochemical Composition

According to the results of the phytochemical GC-MS analysis of the extracts obtained from the aerial parts of both species, *T. occidentalis* comprised 31 compounds (Table 1 and Figure S5), whereas in *P. orientalis*, 33 compounds were identified. These are shown in Table 2 and Figure S6.

Table 1. Chemical composition of the aerial parts extract of *T. occidentalis*.

Retention Time, min	Compound	Relative Abundance (%)
8.7	Terpineol, *cis*-β	0.35
9.8	Eucalyptol	0.25
10.0	L-Fenchone	2.35
10.3	Thujone	16.42
12.0	endo-Borneol	0.85
13.7	1,2,2,3-Tetramethylcyclopent-3-enol	0.78
13.8	γ-Terpineol	0.70
14.9	Bornyl acetate	2.14

Table 1. *Cont.*

Retention Time, min	Compound	Relative Abundance (%)
16.7	α-Terpineol acetate	0.81
16.8	Oxalic acid, 1-menthyl pentyl ester	0.76
17.2	9-Ethylbicyclo(3.3.1)nonan-9-ol	0.40
17.7	Caryophyllene	0.24
23.1	L-Pinocarveol	4.22
27.8	1-Cyclohexanone, 2-methyl-2-(3-methyl-2-oxobutyl)	6.73
30.1	3-*O*-Methyl-D-glucose	17.33
33.4	Cembrene	0.81
34.3	Ambrein	1.91
37.0	Androst-5,16-diene-3β-ol	0.92
37.2	Androst-5-en-17-ol	0.57
37.5	19-Hydroxy-3(α),5-cyclo-5(α)-androstan-17-one	14.53
38.4	Kaurane-16,18-diol, 18-acetate, (4α)-	0.75
38.8	Totarol	7.69
39.1	9-Octadecenamide, (Z)-	0.83
39.2	Ferruginol	1.38
39.3	Kauran-18-oic acid, 16-hydroxy-, (4α)-	0.54
39.4	Podocarp-7-en-3β-ol, 13β-methyl-13-vinyl-	0.69
40.3	Pimaric acid	8.48
40.5	Prasterone	3.16
45.6	Pregnan-20-ol, 3,11-diacetoxy-	1.12
49.6	Vitamin E	2.32

Table 2. Chemical composition of the aerial parts extract of *P. orientalis*.

Retention Time, min	Compound	Relative Abundance (%)
10.0	Fenchone	0.77
10.3	α-Thujone	5.18
15.0	Bornyl acetate	0.44
17.7	Caryophyllene	1.45
18.8	Humulene	1.12
19.7	β-Cubebene	0.85
21.9	Hedycaryol	0.43
22.6	Cubedol	1.19
23.4	Cedrol	0.49
23.8	Epicedrol	5.50
29.5	3-*O*-Methyl-D-glucose	6.98
34.7	Androstenediol	1.97
36.4	Cryptopinon	0.50
37.0	Podocarp-7-en-3β-ol, 13β-methyl-13-vinyl-	5.98
37.7	Prasterone	4.19
38.8	Totarol	4.52
39.2	Ferruginol	1.26
39.4	Pimaric acid	2.82
39.5	β-Pimaric acid	4.58
40.3	Palustric acid	10.19
40.7	5α-Androstane-3β,17β-diol, 17-methyl-	3.84
41.2	Daniellic acid	14.68
41.5	5α-Furost-20(22)-en-26-ol, (25R)-	1.93
44.1	Methandriol	1.47
47.2	Vitamin A_1	13.56

Table 2. *Cont.*

Retention Time, min	Compound	Relative Abundance (%)
47.5	Cyclohexane, 1,3,5-trimethyl-2-octadecylcyclohexane	0.96
48.9	Anthricin	2.65
49.7	Vitamin E	0.48

The chemical composition, along with all detected compounds, their retention times, and relative abundances, are listed in Tables 1 and 2.

As indicated in Table 1, the main components in the extract of *T. occidentalis* include: 3-*O*-methyl-D-glucose (17.33%), followed by thujone (16.42%), 19-hydroxy-3(α)-,5-cyclo-5(α)-androstan-17-one (14.53%), pimaric acid (8.48%), totarol (7.69%), 1-cyclohexanone,2-methyl-2-(3-methyl-2-oxobutyl) (6.73%), and L-pinocarveol (4.22%).

According to the information presented in Table 2, the primary constituents in the extract of *P. orientalis* consist of daniellic acid (14.68%), vitamin A1 (13.56%), palustric acid (10.19%), 3-*O*-methyl-D-glucose (6.98%), podocarp-7-en-3β-ol-,13β-methyl-13-vinyl (5.98%), epicedrol (5.50%), thujone (5.18%), β-pimaric acid (4.58%), totarol (4.52%), and prasterone (4.19%).

Ogunkunle et al. [45] emphasized the use of biochemical parameters to assess the sensitivity and tolerance of species in polluted environments. Terpene compounds, particularly of a terpenoic nature, play a crucial role in plant protection against environmental stresses [46] and are important for allelopathic relationships in plant–plant communication. Volatile terpenes can modulate oxidative stress, signaling, and intercellular reactions with oxidants (such as ozone) induced by abiotic stress, thereby mitigating the effects of oxidative stress. Terpenoids, the main secondary metabolites in *T. occidentalis* and *P. orientalis*, account for a comparable total amount in both species (50.58% and 50.41%, respectively). Examining the composition in detail reveals the presence of abietanes, tricyclic diterpenoids, commonly found in conifer resins, with abietanediterpenecarnosic acid showing potent antioxidant activity [47].

Further analysis indicates that *T. occidentalis* exhibits a slightly higher content of ferruginol and pimaric acid compared to *P. orientalis*, suggesting better antioxidant protection in *T. occidentalis*. Terpenoids significantly contribute to lipid metabolism and accumulation, and the increased content of lipid secondary metabolites (SM) in *T. occidentalis* may explain its superior photosynthetic apparatus performance compared to *P. orientalis*. *T. occidentalis* also shows a higher content of carbohydrates (3-*O*-methyl-D-glucose), further supporting its enhanced photosynthetic activity.

The importance of phytol, a component of chlorophyll; vitamin E; and vitamin K_1 in regards to stress tolerance is evident in the higher vitamin E content in *T. occidentalis* compared to *P. orientalis*. Additionally, *T. occidentalis* exhibits four-fold higher levels of pimaric acid compared to terpenoids. In contrast, *P. orientalis* contains palustric acid and retinol vitamin A_1, suggesting distinct metabolic profiles between the two species.

3.4. Cytotoxic Activity

The study findings related the cytotoxic activity of essential oils derived from *T. occidentalis* and *P. orientalis* are presented in Table 3. The research involved the use of *Artemia salina* L. (Artemiidae), commonly known as brine shrimp larvae. This invertebrate species serves as an alternative test organism to assess the cytotoxicity of both chemical and natural substances, as established by Parra et al. [48].

Table 3. Cytotoxic activity of *T. occidentalis* and *P. orientalis* essential oils.

	Number of Larvae in Control		Number of Larvae in Sample			The Number of Surviving Larvae in the Control	The Number of Surviving Larvae in Sample	Mortality, P	The Percentage of Neurotoxicity
Parallel	**Survived**	**Died**	**Survived**	**Died**	**Paralyzed**	**%**	**%**	**%**	**%**
T. occidentalis									
10 mg/mL									
Medium	24	1	0	26	0	96	0	96	0
5 mg/mL									
Medium	24	1	0	24	0	96	0	96	0
1 mg/mL									
Medium	24	1	4	23	0	96	15	81	0
P. orientalis									
10 mg/mL									
Medium	24	1	0	27	0	96	0	96	0
5 mg/mL									
Medium	24	1	0	25	0	96	0	96	0
1 mg/mL									
Medium	24	1	0	27	0	96	0	96	0

Based on the results from Table 3, the essential oils of *T. occidentalis* and *P. orientalis* demonstrated acute lethal toxicity across all tested concentrations, except for *T. occidentalis* at the lowest concentration of 1 mg/mL, where only one larva survived. Notably, the percentage of mortality was higher in the case of treatment with essential oils of *P. orientalis*. It is crucial to highlight that the increase in mortality is directly proportional to the concentration increase, establishing a linear dose–effect relationship for each sample. This pattern aligns with the findings of the cytotoxicity assay conducted by Parra et al. [48].

Despite both species belonging to the *Cupressaceae* family and containing α-thujone, as indicated in Tables 1 and 2, there is a lack of literature data regarding the examination of *P. orientalis*. Radulović et al. [49] demonstrated a clear correlation between certain essential oil constituents of *T. occidentalis*, other than thujones, and its cytotoxicity. In contrast, the known neurotoxicity of thujones, particularly α-thujone, constituting 51.8% of *T. occidentalis* essential oil, has led to restrictions on their usage in some countries. The essential oils from *T. occidentalis* exhibited significant toxicity towards *A. salina*, surpassing the cytotoxicity of thujone itself, indicating the involvement of other minor constituents in the observed pronounced cytotoxicity [49].

In this study, *T. occidentalis* essential oils exhibited four-fold higher amounts of α-thujone (16.42%) compared to the amounts of α-thujone found in *P. orientalis* (5.18%). Additionally, beyond the *Artemia salina* assay, the literature highlights the cytotoxic activity of *T. occidentalis* and its thujone-rich action against malignant melanoma A375 cancer cells [50]. Furthermore, Torres et al. [51] demonstrated the anti-cancer properties of α/β-thujone against glioblastoma through in vitro and in vivo studies, showing its ability to diminish cell viability, exhibit antiproliferative effects, induce apoptosis, and inhibit angiogenesis. In vivo studies reported the regression of neoplasia and the inhibition of angiogenic markers (VEGF, Ang-4, and CD31) in tumors treated with α/β-thujone [51]. In addition, α-thujone surfaced as a promising terpenoid agent against polycystic ovary syndrome, menstrual problems, and digestive disorders [18], while in traditional medicine, it was used to treat parasitic infections. In conclusion, drawing from the existing literature, it is plausible to suggest that the significant cytotoxicity exhibited by these essential oils against *Artemia salina* may be attributed to the presence of diverse bioactive compounds. For example, terpenes in *Thuja* spp. [52] and phenolics in *Platycladus orientalis* [53,54] are implicated. Both types of compounds have been confirmed to possess antioxidant, antibacterial, antiviral, and anticancer properties. However, further studies are warranted to identify the specific compounds responsible for the cytotoxic effects of these essential oils and to explore their potential applications, particularly in the fields of pharmacology and medicine.

In summary, the existing literature indicates that *Thuja occidentalis* demonstrates tolerance to urban conditions, heat, and drought, although its vitality can be compromised by urban environments and elevated temperatures during mild drought [10,55,56]. Conversely, information on the tolerance of *Platycladus orientalis* to urban conditions, heat, and drought is limited in the available literature [10]. Both species may face vulnerability to climate change, with T. occidentalis showing an unexpected growth decline under warming conditions in North America [57]. However, the specific impacts of climate change on *P. orientalis* remain uncertain. Our study did not observe any signs of tree deterioration or mortality within the studied populations, highlighting the need for further research to elucidate the effects of climate change on both species.

4. Conclusions

In conclusion, our study presents a comprehensive exploration of the physiological, anatomical, and phytochemical characteristics of two widely planted coniferous species, *P. orientalis* and *T. occidentalis*, in the urban environment of Almaty. Our findings shed light on the adaptive mechanisms of *T. occidentalis* to urban stresses, showcasing its greater resilience in anthropogenically transformed conditions within the urban environment. This resilience can be attributed to a combination of factors, including a robust cuticle, well-developed parenchyma cells, submerged stomata, resin passages, and an optimized photosynthetic apparatus, possibly influenced by a more favorable spectrum of synthesized secondary metabolites. Furthermore, our research delved into the chemical composition and cytotoxicity of essential oils derived from *T. occidentalis* and *P. orientalis*. The experimental results unequivocally demonstrate the high cytotoxic activity of the essential oils from both species. This information contributes to the understanding of the pharmacological potential of these essential oils, offering prospects for further exploration in areas such as pharmaceuticals or natural product-based therapies. The link between the physiological characteristics, adaptive mechanisms, and cytotoxic properties provides a holistic perspective on the ecological and pharmacological significance of these coniferous species, emphasizing their multifaceted roles in both urban landscapes and potential therapeutic applications.

Supplementary Materials: The following supporting information can be downloaded at: https://www.mdpi.com/article/10.3390/f15050790/s1, Figure S1. PSII effective quantum yield of photosynthesis (YII) of *T. occidentalis* and *P. orientalis*; data presented are means ± standard error; Figure S2. ETR dynamic of *T. occidentalis* and *P. orientalis*; data presented are means ± standard error; Figure S3. PSII quantum yield of nonregulated energy dissipation (Y(NO)) of *T. occidentalis* and *P. orientalis*; data presented are means ± standard error; Figure S4. PSII quantum yield of regulated energy dissipation (Y(NPQ)) of *T. occidentalis* and *P. orientalis*; data presented are means ± standard error; Figure S5. Chromatographic profile of *T. occidentalis* leaf extract; Figure S6. Chromatographic profile of *P. orientalis* leaf extract.

Author Contributions: Conceptualization, M.K. (Meruyert Kurmanbayeva); methodology, M.K. (Meruyert Kurmanbayeva) and N.T.; software, M.K. (Meruyert Kurmanbayeva), M.R. (Milena Rašeta) and Y.G.; validation, R.J.; formal analysis, N.Y.; investigation, M.Z., M.R. (Milena Rašeta) and Y.G.; resources, M.K. (Meruyert Kurmanbayeva) and N.Y.; data curation, N.Y.; writing—original draft preparation, M.K. (Meruyert Kurmanbayeva), M.Z., M.K. (Marko Kebert), M.R. (Milena Rašeta) and Y.G.; writing—review and editing, N.Y., M.K. (Meruyert Kurmanbayeva), N.T., M.Z., M.K. (Marko Kebert), M.R. (Milena Rašeta), Y.G., R.J. and M.R. (Medeu Razhanov); visualization, M.Z. and Y.G.; supervision, M.K. (Meruyert Kurmanbayeva); project administration, M.K. (Meruyert Kurmanbayeva); funding acquisition, N.Y. All authors have read and agreed to the published version of the manuscript.

Funding: This research was funded by the Ministry of Science and Higher Education of the Republic of Kazakhstan (Grant No. BR21882122).

Data Availability Statement: Data are contained within the article.

Conflicts of Interest: The authors declare no conflicts of interest.

References

1. Zhang, B.; Brack, C.L. Urban forest responses to climate change: A case study in Canberra. *Urban For. Urban Green.* **2021**, *57*, 126910. [CrossRef]
2. Sharma, A.; Andhikaputra, G.; Wang, Y.C. Heatwaves in South Asia: Characterization, consequences on human health, and adaptation strategies. *Atmosphere* **2022**, *13*, 734. [CrossRef]
3. Ulpiani, G. On the linkage between urban heat island and urban pollution island: Three-decade literature review towards a conceptual framework. *Sci. Total Environ.* **2021**, *751*, 141727. [CrossRef]
4. Percival, G.C. Heat tolerance of urban tree species-a review. *Urban For. Urban Green.* **2023**, *86*, 128021. [CrossRef]
5. Bialecki, M.B.; Fahey, R.T.; Scharenbroch, B. Variation in urban forest productivity and response to extreme drought across a large metropolitan region. *Urban Ecosyst.* **2018**, *21*, 157–169. [CrossRef]
6. Abdollahi, P.; Soltani, A.; Beigi Harchegani, H.A. Evaluation of salinity tolerance in four suitable tree species in urban forestry. *Iran. J. For. Poplar Res.* **2011**, *19*, 265–282. [CrossRef]
7. Shabanian, N.; Cheraghi, C. Comparison of phytoremediation of heavy metals by woody species used in urban forestry of Sanandaj city. *Iran. J. For. Poplar Res.* **2013**, *21*, 154–165. [CrossRef]
8. Škrbić, B.; Đurišić-Mladenović, N.; Živančev, J.; Tadić, Đ. Seasonal occurrence and cancer risk assessment of polycyclic aromatic hydrocarbons in street dust from the Novi Sad city, Serbia. *Sci. Total Environ.* **2019**, *647*, 191–203. [CrossRef]
9. Yousofpour, Y.; Abolhassani, L.; Hirabayashi, S.; Burgess, D.; Sabouni, M.S.; Daneshvarkakhki, M. Ecosystem services and economic values provided by urban park trees in the air polluted city of Mashhad. *Sustain. Cities Soc.* **2024**, *101*, 105110. [CrossRef]

10. Kerimray, A.; Azbanbayev, E.; Kenessov, B.; Plotitsyn, P.; Alimbayeva, D.; Karaca, F. Spatiotemporal variations and contributing factors of air pollutants in Almaty, Kazakhstan. *Aerosol Air Qual. Res.* **2020**, *20*, 1340–1352. [CrossRef]
11. Bočkova, S.; Bohovic, R.; Hrnčiar, M.; Muroň, M.; Chytrý, J.; Skalský, M.; Černochová, M.; Kalmykov, D. *Air Pollution in Kazakhstan as Seen from Space: Fundamental Analysis, Focus on the Karaganda Region, and Notes on Kazakhstan's Broader Impact on Climate Change*; Labohy, J., Ed.; World from Space: Brno, Czech Republic, 2023; ISBN 978-80-88508-16-8.
12. Rahmonov, O.; Pukowiec-Kurda, K.; Banaszek, J.; Brom, K. Floristic diversity in selected city parks in southern Poland. *Ochr. Sr. I Zasobow Nat.* **2020**, *30*, 8–17. [CrossRef]
13. Ahn, J.W.; Dinh, T.V.; Park, S.Y.; Choi, I.Y.; Park, C.R.; Son, Y.S. Characteristics of biogenic volatile organic compounds emitted from major species of street trees and urban forests. *Atmos. Pollut. Res.* **2022**, *13*, 101470. [CrossRef]
14. Zorić, M.; Kostić, S.; Kladar, N.; Božin, B.; Vasić, V.; Kebert, M.; Orlović, S. Phytochemical screening of volatile organic compounds in three common coniferous tree species in terms of forest ecosystem services. *Forests* **2021**, *12*, 928. [CrossRef]
15. Antonelli, M.; Donelli, D.; Barbieri, G.; Valussi, M.; Maggini, V.; Firenzuoli, F. Forest volatile organic compounds and their effects on human health: A state-of-the-art review. *Int. J. Environ. Res. Public Health* **2020**, *17*, 6506. [CrossRef]
16. Kebert, M.; Kostić, S.; Rašeta, M.; Stojanović, D.V.; Stojnić, S.; Orlović, S. Species-specific level variation in polyamines in coniferous and deciduous woody plant species in urban areas. *Horticulturae* **2023**, *9*, 1157. [CrossRef]
17. McPherson, E.G.; Berry, A.M.; van Doorn, N.S. Performance testing to identify climate-ready trees. *Urban For. Urban Green.* **2018**, *29*, 28–39. [CrossRef]
18. Skok, A.V. Assessment of ecological condition of coniferous plants in the urbanized territory. *Perm Agrar. J.* **2018**, *21*, 155–159.
19. Pudełek, M.; Catapano, J.; Kochanowski, P.; Mrowiec, K.; Janik-Olchawa, N.; Czyż, J.; Ryszawy, D. Therapeutic potential of monoterpene α-thujone, the main compound of *Thuja occidentalis* L. essential oil, against malignant glioblastoma multiforme cells in vitro. *Fitoterapia* **2019**, *134*, 172–181. [CrossRef]
20. Akkol, E.K.; İlhan, M.; Demirel, M.A.; Keleş, H.; Tümen, I.; Süntar, İ. *Thuja occidentalis* L. and its active compound, α-thujone: Promising effects in the treatment of polycystic without inducing osteoporosis. *J. Ethnopharmacol.* **2015**, *168*, 25–30. [CrossRef]
21. Rehman, R.; Zubair, M.; Bano, A.; Hewitson, P.; Ignatova, S. Isolation of industrially valuable α-cedrol from essential oil of *Platycladus orientalis* (*Thuja orientalis*) leaves using linear gradient counter current chromatography. *Ind. Crops Prod.* **2022**, *176*, 114297. [CrossRef]
22. Alves, L.D.S.; Figueirêdo, C.B.M.; Silva, C.C.A.R.; Marques, G.S.; Ferreira, P.A.; Soares, M.F.R.; Silva, R.M.; Rolim-Neto, P.J. *Thuja occidentalis* L. (Cupressaceae): Review of botanical, phytochemical, pharmacological and toxicological aspects. *Int. J. Ppharm. Sci. Res.* **2014**, *5*, 1163. [CrossRef]
23. Stein, R.A.; Sheldon, N.D.; Smith, S. Rapid response to anthropogenic climate change by *Thuja occidentalis*: Implications for past climate reconstructions and future climate predictions. *PeerJ* **2019**, *7*, e7378. [CrossRef]
24. Cui, N.; Qu, L.; Wu, G. Heavy metal accumulation characteristics and physiological response of *Sabina chinensis* and *Platycladus orientalis* to atmospheric pollution. *J. Environ. Sci.* **2022**, *112*, 192–201. [CrossRef]
25. Safaralie, A.; Fatemi, S.; Salimi, A. Experimental design on supercritical extraction of essential oil from valerian roots and study of optimal conditions. *Food Bioprod. Process.* **2010**, *88*, 312–318. [CrossRef]
26. Rahmani, F.; Sodaeizadeh, H.; Yazdani-Biouki, R.; Hakimzadeh-Ardakani, M.A.; Aliabadi, K.K. Effect of bio-priming on morphological, physiological and essential oil of Chamomile (*Matricaria chamomilla* L.) under salinity stress. *S. Afr. J. Bot.* **2024**, *167*, 630–642. [CrossRef]
27. Kumar, D.; Punetha, A.; Khan, A.; Suryavanshi, P.; Yogendra, N.D.; Padalia, R.C. Assessment of soil moisture stress induced variability in oil content and composition in mint species. *Biochem. Syst. Ecol.* **2024**, *113*, 104774. [CrossRef]
28. Viladomat, F.; Bastida, J. General overview of plant secondary metabolism. In *Plant Biology and Biotechnology*; Volume I: Plant Diversity, Organization, Function and Improvement; Springer: Berlin/Heidelberg, Germany, 2015; pp. 539–568. [CrossRef]
29. Atkinson, N.J.; Urwin, P.E. The interaction of plant biotic and abiotic stresses: From genes to the field. *J. Exp. Bot.* **2012**, *63*, 3523–3543. [CrossRef]
30. Starikova, E.A.; Voskresenskaja, O.L.; Sarbaeva, E.V. Change of a pigmentary complex of a fir-tree prickly in the conditions of the urban environment. *Int. Sci. Res. J.* **2016**, *10*, 46–48.
31. Sperdouli, I.; Moustaka, J.; Ouzounidou, G.; Moustakas, M. Leaf age-dependent photosystem II photochemistry and oxidative stress responses to drought stress in Arabidopsis thaliana are modulated by flavonoid accumulation. *Molecules* **2021**, *26*, 4157. [CrossRef]
32. Chakraborty, S.; Afaq, N.; Singh, N.; Majumdar, S. Antimicrobial activity of *Cannabis sativa*, *Thuja orientalis* and *Psidium guajava* leaf extracts against methicillin-resistant *Staphylococcus Aureus*. *J. Integr. Med.* **2018**, *16*, 350–357. [CrossRef]
33. Figueiredo, C.B.M.; Alves, L.D.S.; Silva, C.C.A.R.; Ferreira, P.A.; Marques, G.S.; Santana, A.S.C.O.; Randau, K.P.; Pimentel, R.M.M.; Silva, R.M.F.; Rolim-Neto, P.J. Physical-chemical characterization, anatomical and seasonal evaluation of *Thuja occidentalis* L. (Cupressaceae). *Int. J. Pharm. Sci. Res.* **2014**, *5*, 1721–1731. [CrossRef]
34. Wang, R.; Nie, L.; Zhang, S.; Cui, Q.; Jia, M. Research progress on plant resistance to heavy metal stress. *Acta Hortic. Sin.* **2019**, *46*, 157–170. [CrossRef]
35. Hoffmann, N.; Schall, P.; Ammer, C.; Leder, B.; Vor, T. Drought sensitivity and stem growth variation of nine alien and native tree species on a productive forest site in Germany. *Agric. For. Meteorol.* **2018**, *256*, 431–444. [CrossRef]

36. Agarwal, P.; Sarkar, M.; Chakraborty, B.; Banerjee, T. Phytoremediation of air pollutants: Prospects and challenges. In *Phytomanagement of Polluted Sites*; Elsevier: Amsterdam, The Netherlands, 2019; Volume 7, pp. 221–241. [CrossRef]
37. González, M.C.; Cejudo, F.J.; Sahrawy, M.; Serrato, A.J. Current knowledge on mechanisms preventing photosynthesis redox imbalance in plants. *Antioxidants* **2021**, *10*, 1789. [CrossRef]
38. Czarnocka, W.; Karpiński, S. Friend or foe? Reactive oxygen species production, scavenging and signaling in plant response to environmental stresses. *Free Radic. Biol. Med.* **2018**, *122*, 4–20. [CrossRef]
39. Agathokleous, E.; Kitao, M.; Calabrese, E.J. Hormesis: A compelling platform for sophisticated plant science. *Trends Plant Sci.* **2019**, *24*, 318–327. [CrossRef]
40. Tyystjärvi, E. Photoinhibition of photosystem II. *Int. Rev. Cell Mol. Biol.* **2013**, *300*, 243–303. [CrossRef] [PubMed]
41. Adamakis, I.D.S.; Sperdouli, I.; Eleftheriou, E.P.; Moustakas, M. Hydrogen peroxide production by the spot-like mode action of bisphenol A. *Front. Plant Sci.* **2020**, *11*, 1196. [CrossRef]
42. Adamakis, I.D.S.; Sperdouli, I.; Hanć, A.; Dobrikova, A.; Apostolova, E.; Moustakas, M. Rapid hormetic responses of photosystem II photochemistry of clary sage to cadmium exposure. *Int. J. Mol. Sci.* **2020**, *22*, 41. [CrossRef]
43. Ruban, A.V. Nonphotochemical chlorophyll fluorescence quenching: Mechanism and effectiveness in protecting plants from photodamage. *Plant Physiol.* **2016**, *170*, 1903–1916. [CrossRef]
44. Orekhov, D.I.; Yakovleva, O.V.; Goryachev, S.N.; Protopopov, F.F.; Alekseev, A.A. The use of parameters of chlorophyll a fluorescence induction to evaluate the state of plants under anthropogenic load. *Biophysics* **2015**, *60*, 263–268. [CrossRef]
45. Ogunkunle, C.; Oyedeji, S.; Adeniran, I.F.; Olorunmaiye, K.S.; Fatoba, P.O. *Thuja occidentalis* and *Duranta repens* as indicators of urban air pollution in industrialized areas of southwest Nigeria. *Agric. Conspec. Sci.* **2019**, *84*, 193–202.
46. Boncan, D.A.T.; Tsang, S.S.; Li, C.; Lee, I.H.; Lam, H.M.; Chan, T.F.; Hui, J.H. Terpenes and terpenoids in plants: Interactions with environment and insects. *Int. J. Mol. Sci.* **2020**, *21*, 7382. [CrossRef] [PubMed]
47. Novoa, M.L.; Escalante, Y.; Maldonado, L.; Galindo-Castro, I.; Álvarez, A.; Figarella, K.; Villamizar, J.E. Synthesis and bio-logical evaluation of (−)-13, 14-dihydroxy-8, 11, 13-podocarpatrien-7-one and derivatives from (+)-manool. *Nat. Prod. Res.* **2015**, *29*, 207–212. [CrossRef] [PubMed]
48. Parra, A.L.; Yhebra, R.S.; Sardiñas, I.G.; Buela, L.I. Comparative study of the assay of *Artemia salina* L. and the estimate of the medium lethal dose (LD_{50} value) in mice, to determine oral acute toxicity of plant extracts. *Phytomedicine* **2001**, *8*, 395–400. [CrossRef]
49. Radulović, N.S.; Gencic, M.; Stojanović, N.M.; Randjelović, P.J.; Stojanović-Radić, Z.Z.; Stojiljković, N. Toxic essential oils. Part V: Behaviour modulating and toxic properties of thujones and thujone-containing essential oils of *Salvia officinalis* L., *Artemisia absinthium* L., *Thuja occidentalis* L. and *Tanacetum vulgare* L. *Food Chem. Toxicol.* **2017**, *105*, 355–369. [CrossRef]
50. Biswas, R.; Mandal, S.K.; Dutta, S.; Bhattacharyya, S.S.; Boujedaini, N.; Khuda-Bukhsh, A.R. Thujone-rich fraction of Thuja occidentalis demonstrates major anti-cancer potentials: Evidences from in vitro studies on A375 cells. *J. Evid. Based Complement. Altern. Med.* **2011**, *2011*, 568148. [CrossRef] [PubMed]
51. Torres, A.; Vargas, Y.; Uribe, D.; Carrasco, C.; Torres, C.; Rocha, R.; Oyarzun, C.; Martin, R.S.; Quezada, C. Pro-apoptotic and anti-angiogenic properties of the α/β-thujone fraction from Thuja occidentalis on glioblastoma cells. *J. Neurooncol.* **2016**, *128*, 9–19. [CrossRef] [PubMed]
52. Malhocká, A.; Švábová, M. Diversity of the terpene synthesis in the *Thuja* species—A comparative chemotaxonomic study. *Biochem. Syst. Ecol.* **2023**, *110*, 104703. [CrossRef]
53. Hashemi, S.M.; Safavi, S.A. Chemical constituents and toxicity of essential oils of oriental *Arborvitae*, *Platycladus orientalis* (L.) Franco, against three stored-product beetles. *Chilean J. Agric. Res.* **2012**, *72*, 188–194. [CrossRef]
54. Khammassi, M.; Ayed, R.B.; Khedhiri, S.; Souihi, M.; Hanana, M.; Amri, I.; Hamrouni, L. Crude extracts and essential oil of *Platycladus orientalis* (L.) Franco: A source of phenolics with antioxidant and antibacterial potential as assessed through a chemometric approach. *Turk. J. Agric. For.* **2022**, *46*, 477–487. [CrossRef]
55. Zhao, J.; Hartmann, H.; Trumbore, S.E.; Ziegler, W.; Zhang, Y. High temperature causes negative whole-plant carbon balance under mild drought. *New Phytol.* **2013**, *200*, 330–339. [CrossRef] [PubMed]
56. Kycheryavyi, V.; Popovych, V.; Dyda, O.; Shuplat, T.I.; Bosak, P. The Influence of climatic and edaphic conditions on the development of *Thuja occidentalis* 'Smaragd' under the urban conditions of a large city. *J. Ecol. Eng.* **2021**, *22*, 325–332. [CrossRef]
57. Housset, J.M.; Girardin, M.P.; Baconnet, M.; Carcaillet, C.; Bergeron, Y. Unexpected warming-induced growth decline in *Thuja occidentalis* at its northern limits in North America. *J. Biogeogr.* **2015**, *42*, 1233–1245. [CrossRef]